

# A Novel Cardiac Auscultation Monitoring System Based on Wireless Sensing for Healthcare

HAORAN REN<sup>1</sup>, HAILONG JIN<sup>2</sup>, CHEN CHEN<sup>1</sup>, HEMANT GHAYVAT<sup>1</sup>,  
AND WEI CHEN<sup>1,3</sup>, (Senior Member, IEEE)

<sup>1</sup>Center for Intelligent Medical Electronics, School of Information Science and Technology, Fudan University, Shanghai 200433, China

<sup>2</sup>Department of Biomedical Engineering, School of Electrical Engineering, Yanshan University, Qinhuangdao 066004, China

<sup>3</sup>Shanghai Key Laboratory of Medical Imaging Computing and Computer Assisted Intervention, Fudan University, Shanghai 200433, China

CORRESPONDING AUTHOR: W. CHEN (w\_chen@fudan.edu.cn)

This work was supported in part by the National Key R&D Program of China under Grant 2017YFE0112000 and in part by the Shanghai Municipal Science and Technology Major Project under Grant 2017SHZDZX01.

**ABSTRACT** Heart sounds deliver vital physiological and pathological evidence about health. Wireless cardiac auscultation offers continuous cardiac monitoring of an individual without 24\*7 manual healthcare care services. In this paper, a novel wireless sensing system to monitor and analyze cardiac condition is proposed, which sends the information to the caregiver as well as a medical practitioner with an application of the Internet of Things (IoT). An integrated system for heart sound acquisition, storage, and asynchronous analysis has been developed, from scratch to information uploading through IoT and signal analysis. Cardiac auscultation sensing unit has been designed to monitor cardiovascular health of an individual. Bluetooth protocol is used to offer power efficiency and moderate data transmission rate. The Hilbert–Huang transform is used to eliminate interference signals and to help to extract the heart sound signal features. Subsequence segmentation algorithm based on double-threshold has been developed to extract physiological parameters. Preprocessing, segmentation, and clustering technique were performed for significant health information interpretation. The cardiac auscultation monitoring system may provide a way for heart disease self-management.

**INDEX TERMS** Heart sound, IoT, Hilbert-Huang transform, double-threshold.

## I. INTRODUCTION

The strategy of physiological measurement systems has been a mounting research attention in the last decade, due to the possible applications in medicine, sports, and security. With the growth in the proportions of the adult and elderly population, as well as the emergence of chronic diseases and syndromes because of the ups and downs in lifestyle, there has been a necessity to monitor and analyze the health status of individuals in their daily living to avoid fatal conditions. The adoption of wireless health monitoring is encouraging to boost the quality of lifespan for chronic sick patients and the old people, as well as healthy one [1]–[4]. Moreover, unnecessary hospitalizations can be avoided by the remote health monitoring which reduces the cost of care and increases the quality of care [5]–[7]. The long-term monitoring of physical activity facilitates the development of interdisciplinary healthcare research [8]. The transformation of healthcare, evolving from traditional health management to more

personalized healthcare systems with the application of the Internet of Things, benefits the personal health [9].

Cardiovascular disease is one of the major health problems and a leading cause of mortality around the world [10]. The electrocardiogram (ECG), which is the most popular method for checking cardiac anomaly function works by detecting the electrical signals. While the heart disorder caused by structure abnormalities are more likely to produce mechanical vibrations other than electrical ones [11]. Heart auscultation which is popular in clinics has been a very important method for the early diagnosis of heart disease by capturing cardiac murmurs. Cardiac murmurs can expose many pathological cardiac defects such as heart failure, arrhythmia, valve disease, cardiomyopathy, etc. The heart sound signal contains a lot of heart information, giving a preliminary suggestion for further diagnosis. While the auscultation of the heart sound is very subjective, and it largely depends on the experience, skills, and hearing ability of the physician [12]. What's more,

without software to record the patients' heart sounds, it is difficult for cardiologists to capture heart sounds which are a rare occurrence and to know the evolution of heart disease. Continuous health monitoring can provide long-term information about the evolution of physiological indicators. Taking these aspects into consideration, it is necessary to improve the technology of stethoscope, and the benefits of the electronic stethoscope can be considerable.

Electronic stethoscope makes heart auscultation more convenient. Many experts have made some researches to detect and analyze the heart sound, specifically the design of new sensors and the algorithm analysis methods. The sensors in electronic stethoscopes vary widely, such as a microphone, piezoelectric sensors, and capacity type sensors, etc. [13]. Many researchers have used different materials and technologies in heart sound sensors [14]–[17]. The most widely used material of heart sound sensor is piezoelectric. From an engineering perspective, there are three steps for automated analysis of the heart sound, namely, preprocessing, feature extraction and classification. Many types of research concentrated on the methods of segmentation and classification of heart sounds. Hilbert-Huang transform was used to analyze Coronary Artery Disease [18]. Trimmed mean spectrogram method was used to extract heart sound signals features [19]. Hidden Markov Model was used to build a classification model for heart murmur recognition [20]. Most of the researchers have done systematically based on laboratory environment and offered high precision and accuracy. These researches fail to offer reasonable accuracy in real-world uncontrolled conditions.

Moreover, there are many commercial devices. 3M Littmann [21] and Thinkslabs Medical company [22] have introduced the finest electronic stethoscope using the Ambient Noise Reduction (ANR) technology to reduce the unwanted background noise, and the amplification ability is far superior to the conventional stethoscope. Besides, some commercial devices reduced the ambient noise using the basic band pass filtering mechanism or special sensor structure design. However, the cost of the 3M Littmann Cardiology stethoscope is around \$200 and the regular price of the high-end device (i.e., 3M Littmann 4100WS) is \$869 which is not affordable for the ordinary family [23]. Additionally, the commercial products have been focused on the data collecting, the accuracy of classification has not been reported [13].

At present, cardiac auscultation devices mainly collect signals through heart sound sensors and then transmit to a computer which acts as a display device and analyzes the heart sound for further research. It is inconvenient for users in daily life [24], [25]. Although the existing commercial digital stethoscopes have many advantages over the traditional stethoscope, we cannot deny the fact that the cost for a digital stethoscope is high.

This research presents a cardiac acquisition monitoring system which takes the advantages of wireless technology, implemented via Bluetooth technology, and computational

methods of diagnosis of heart physiology. With the application of the Internet of Things, the users or doctors can get the instant status of heart and take clinical interference before an emergency. The latest Bluetooth 4.0 is chosen as the version of Bluetooth module, which has the characteristics of low power consumption, small in size and moderate data rate in the ISM band RF radio families. Thus, the abilities of portable, power efficiency, simplify operation, and cost efficiency makes the hardware prototype more acceptable for customers. What's more, the price of the proposed system would be much lower if produced in large scale. The heart sound data is transmitted wirelessly to an Android smartphone for visual display which helps people obtain the intuitive information. On the signal processing aspect, the EMD method is recruited to eliminate noises effectively involving the ambient noise, friction noise which is induced by the body movement. Additionally, the integration of the Hilbert-Huang transform and double-threshold method is used to realize preprocessing and to extract useful physiological parameters from heart sounds. Furthermore, the features are compared in the time domain and frequency domain, which provides a way to distinguish the differences between normal and anomalous heart sounds.

The paper is organized as follows: the theory of heart auscultation consisting cardiac auscultation area and characteristics of heart sound is mainly introduced in Section II. The detailed information including methodology, system architecture, hardware design, smartphone application interface and analysis of algorithm is given in Section III. The experiments and results based on the signal processing are drawn in Section IV. Discussion and Conclusion are described in Section V and VI, respectively.

## II. HEART AUSCULTATION

During the cardiac cycle, the electrical activation of the heart is the first action, which then leads to the contraction of the atrial and ventricular forming a mechanical activity. The mechanical activity followed by the opening and closure of the heart valves, forcing the sudden start or stop of the flow of blood. The result of the above action forms vibrations of the entire cardiac structure [26]. These vibrations are audible on the chest wall, which has four locations: Aortic area, Pulmonic area, Tricuspid area and Mitral area [27]. The locations were marked in Fig.1. The stethoscope was positioned in the mitral area where the heart sounds were best heard.

Heart sound is complex and non-stationary in nature. The normal heart sound typically has two components: the first heart sound (S1) and the second heart sound (S2). S1 occurs at the beginning of ventricular contraction initiated by the closure of the atrioventricular valves. S2 occurs at the beginning of ventricular diastole initiated by the closure of the semilunar valve. While S1 and S2 are outstanding sound during the cardiac cycle, many other audible sounds may occur due to the pathological or physiological features, such as the third (S3) and the fourth (S4) heart sound. However, most researchers will select the S1 and S2 as research targets,

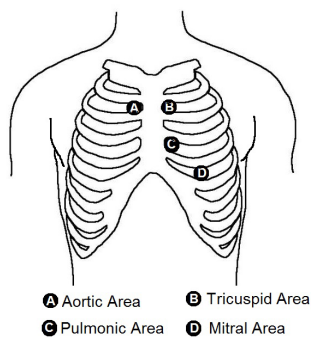


**FIGURE 1.** Cardiac auscultation areas.

because S3 and S4 appear at very low amplitudes with low-frequency components and are difficult to be caught in usual auscultation.

The frequency of normal heart sound mainly concentrated in 20-150Hz. In the case of pathology, the heart sound contains high-frequency murmurs which are generally higher than the normal heart sound frequency, concentrated in the range of 100-600Hz, some of them up to 1000Hz. In the normal heart, the physiological changes, such as heart murmurs, are produced by spray blood speed. In impaired heart and vascular, myocardial contraction force changes, heart valve mouth narrow or closed incomplete, or heart blood flow velocity changes, all can make obvious changes of the amplitude or frequency of the heart diastolic activity, also can produce anomaly heart sound or heart murmur. These changes will help clinicians to diagnose cardiac vascular disease, observe the changes of patients' condition, and estimate prognosis, etc.

Designing a wireless system for health monitoring is a very burdensome assignment. There are many key concerns to be addressed, including:

- designing trustworthy sensor and sensing unit;
- ensuring the consistent signal transmission of cardiac auscultation sign;
- providing authentication and authorized access to ensure the security and privacy of user data.

Remote transmission is both a key benefit of such systems and a constraint on their design as well. To accomplish this benefit, wireless physiological sensors must be small, lightweight and power efficient. The next section illustrates the system proposal and prototype designing.

### III. SYSTEM DESIGN AND IMPLEMENTATION

#### A. SYSTEM DESIGN

Considering the main users and application scenarios, the system should be portable and simplify the control of the application. A completed cardiac auscultation monitoring system includes acquisition module embedded with heart sound sensor, a display unit and analysis system with the function of feedback. The concept design of the monitoring system is shown in Fig.2. The acquisition module consists of

a microcontroller and a Bluetooth 4.0 unit, which samples the heart sound signals and transmits the data to the mobile phone which is embedded with Bluetooth 4.0 also. The capabilities of widespread use and low energy of Bluetooth 4.0 improve the compatibility and decrease the power consumption of this system. Subsequently, the Android cell phone receives the heart sound data and plots the signal curves in real-time. The mobile application acts as the display device and has the capability to upload data to a cloud platform for further analysis. The cloud platform integrates the data for concentrated processing and storage. Consequently, the authorized pathologists and doctors can get access to the cloud platform to get the dataset and results via any peripheral devices which are equipped with specific software. Moreover, the users can obtain the diagnose results, and the proposed system realize the telemedicine eventually.

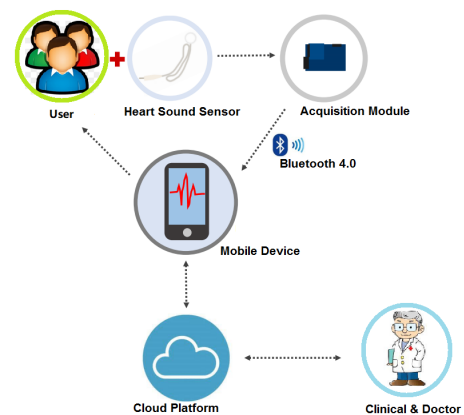


**FIGURE 2.** System architecture.

#### B. PROTOTYPE

The diagram of the proposed system is shown in Fig. 3. Sensing module which is mainly composed of heart sound sensor and control module, realizes raw data collection and the transmission of heart sound signals. The signal is transmitted to an Android phone via Bluetooth 4.0 module. The Android application is designed to complete the data reception and visualization. The analysis system is responsible for analyzing the heart sound, which includes signal pre-processing, feature extraction and data clustering. The heart sound signal is susceptible to the environmental interference, so it is important to select a suitable sensor. In this paper, the HKY-06B heart sound sensor which is manufactured by Huake electronic takes the weak heart vibration signal into electrical signals [28]. This heart sound sensor integrated with micro-sound components are made from polymer materials. It has the capability to detect all kinds of heart sound and acoustic sound on the body surface. The specification of the heart sound sensor is shown in Table 1.

Even though there are kinds of wireless technologies, the trade-off between the various solutions should be considered.

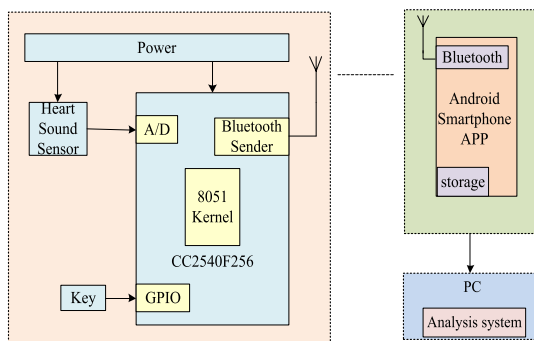


FIGURE 3. The structure diagram of the monitoring system.

TABLE 1. The specification of the heart sound sensor.

Heart sound sensor (HKY-06B)	
Voltage VCC	3V~6V
Current	5mA
Frequency	1Hz~1500Hz
Sensitive	4mV/Pa
Output amplitude	0.5V~1.5V

Compared with other wireless technologies, like Zigbee and Wi-Fi, Bluetooth 4.0 has many advantages. The most appealing features are low energy and fairly simple to use. Unlike Wi-Fi which is more complex and requires configuration of software and hardware, Bluetooth can be used to connect multi-peripheral devices at a time. As for the data transfer speed, Bluetooth 4.0 is enough for the transfer of physiological signals. Although the mesh network of Zigbee allows devices to work in the complex system, Zigbee does not support by Android or iOS. In this paper, the data acquisition module is controlled by the CC2540 unit, which contains a CC2540 system-on-chip, an external antenna, and other auxiliary components. The tasks of the control unit are A/D sampling, controlling GPIO and Bluetooth transmission. The chip of CC2540 which is produced by Texas Instruments integrates an 8051-based micro-controller with 8kB RAM and a BLE transceiver operating in the 2.4GHz frequency band. It also has an internal 8-channel ADC converter, which can be configured the resolution, ranging from 8 to 14 bits. What's more, the integration of the USB would allow engineers to take advantage of the integrated application. In this paper, the A/D sampling rate is set at 1 kHz with 12-bit. And the A/D sampling was triggered by Timer 3 which is an 8-bit timer with timer/counter/PWM functionality. The external antenna only needs a few simple RC network which can be realized complex RF front-end, and this part of the circuit is called Balun matching circuit. The key integrated on the acquisition module is used to control the start of the system by controlling the function of the timer. The sensing module is shown in Fig. 4.

CC2540 chip was equipped with a BLE protocol stack provided by Texas Instruments. The software architecture of

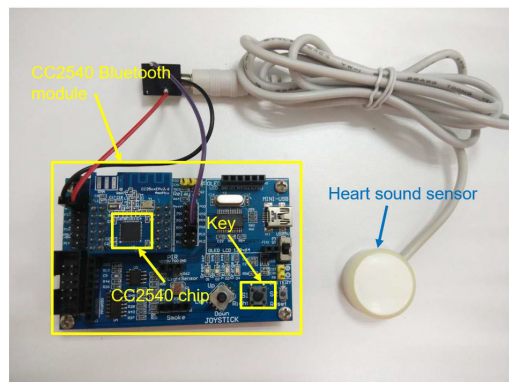


FIGURE 4. The acquisition module and the heart sound sensor.

the CC2540 is based on the Operating System Abstraction Layer (OSAL), which is not an actual operating system (OS) in the traditional sense, but rather a control loop that allows software to set up execution of events [29].

In this system, the sensing module acts as the peripheral station and the local home gateway as the central station. The local home gateway system takes the role of Generic Attribute Profile (GATT) server and executes the service which contains seven Characteristics. The system uses the seventh characteristic CHAR7 to complete the data transmission, which is a periodic notification mode. When the server data changes, the client obtains CHAR7 notification instead of reading the data. According to the CC2540 transmission format, the length of the payload is 20-byte. Therefore, the heart sound should be collected for ten times, and then transmit them to a smartphone through the notification of CHAR7.

The process for building the cardiac acquisition system is in a deliberate, structured and methodical way. What's more, the accuracy of the signals which were collected through CC2540 was calibrated by packet loss rate (PLR) and received signal strength indicator (RSSI). The signal transmission quality in different communication range was tested. The results showed that the PLR was zero when the communication range is less than 10 meters.

### C. APPLICATION INTERFACE

In particular, the usage of the mobile phones covers everywhere around the globe with an open platform. The Android application was developed and tested using a XiaoMi 3 smartphone with Android 4.3 which runs atop the Linux kernel from Google. A typical Android application consists of four components: Activities, Services, Broadcast Receivers and Content providers. The Eclipse development platform is used to design the user interface by using Android API and the application (App) is programmed by Java language. In this paper, the mobile application was designed to display and store the heart sounds (physiological data). The smartphone acts as a central station and provides a user interface. The tasks of the application are to receive the sensor information

collected from acquisition system, display the heart sound waveform in real-time, store data and review historical data. The App is composed of nine Java files which are shown in Fig. 5.

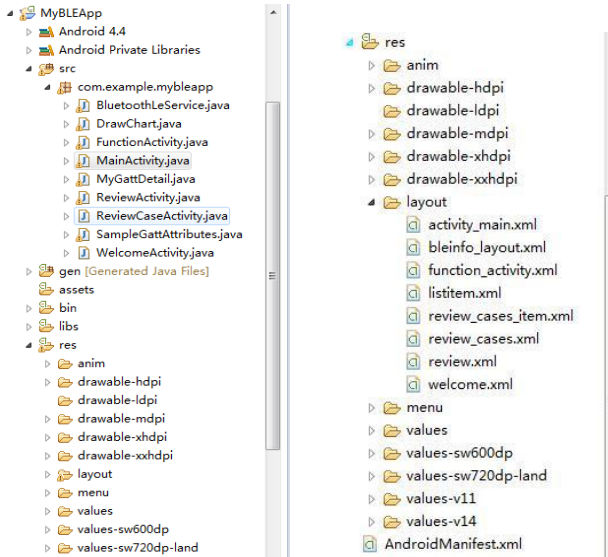


FIGURE 5. Java files of the APP.

The picture shown in the first column exhibits 9 Java class file, which contains BluetoothLeService, DrawChart, FunctionActivity, MainActivity, etc. These classes are Service class, View class or Activity class, which are used for configuration and interface display. The picture shown in the second column indicates that the 'res' folder stores the resource files (e.g., \*.png, \*.jpg) and description file.

### 1) BLUETOOTH DEVICE SCAN

To use the Bluetooth function in the APP, the Bluetooth permission must be declared in AndroidManifest.xml which is the automatically generated description file. In addition to the configuration of the Bluetooth permission, uses-feature also need to be declared. When the application starts, the BLE device begins to discover peripheral devices. The device discovery process is done through the startLeScan() method. The name of each BLE device found is stored in LeDeviceListAdapter, along with their MAC addresses. The BLE devices list is shown in Fig.6 a). The results of peripheral devices are shown in "MainActivity" which is the main Activity of the application program.

### 2) DATA TRANSMISSION AND WAVEFORM DISPLAY

After searching tasks, a peripheral device should be selected and establish the connection to the central device. In this system, smartphone act as a GATT client, and the acquisition module as a GATT server. The first step to communicate with the device is to connect the GATT client with the GATT server, which is done using the connectGatt() method.

The activity "MyGattDetail" was defined to receive data from acquisition module, present multiple Services and

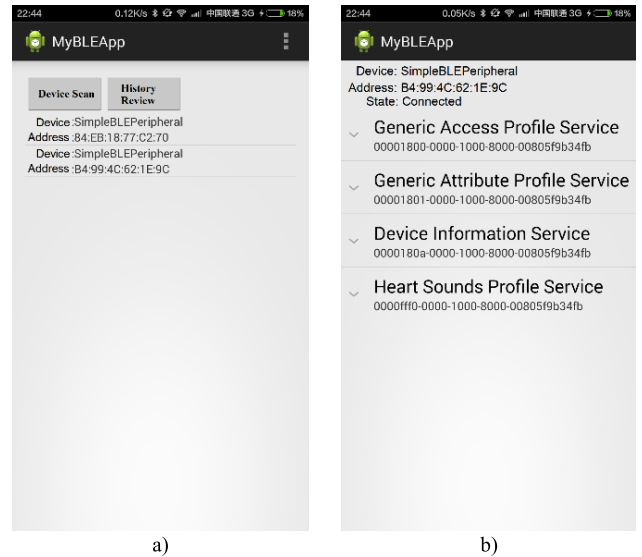


FIGURE 6. The list of BLE devices and profile services. a) BLE device list. b) Device information.

exhibit Characteristics supported by the BLE device. The device information interface is shown in Fig.6 b). The accessible services and Characteristics were added to Expandable ListView which bound with a Click event listener. When the "Heart sound profile service" was selected, the drop-down list would show all the Characteristics of the service, ranging from fff1 to fff7. The seventh characteristic containing the heart sound data which was in ASCII format, need to be converted to hexadecimal, and then added to the data buffer.

### 3) DATA STORAGE AND HISTORICAL REVIEW

When the data is stored in the drawing buffer, the view is regularly updated to realize delineating the heart sound waveform in real-time. The waveform drawing interface is shown in Fig. 7, which contains the device connection status, the content of the received data and the signal curve.

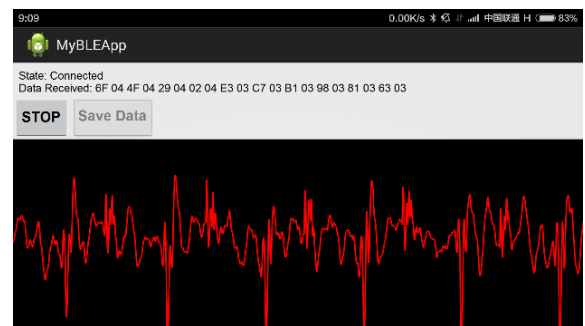


FIGURE 7. Heart sound waveform in real-time.

In order to realize further research, the application has the capacity to store heart sound data. Before storing data, the permission to read and write should be declared. If the storage is supported, the data will be stored in a specified directory path. The history recording is shown in Fig. 8.

The picture shown in the first column is a screenshot from Eclipse which exhibits the file folders on the Android phone. The historical review of the collected data (second column) is named by the timestamp.

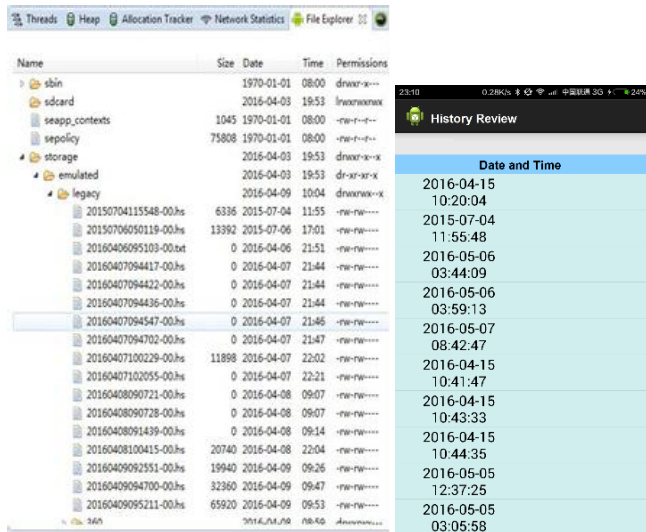


FIGURE 8. History recording.

Before storing the file, the data format should be converted to a binary format for subsequent reading operations, then the data was saved to the specified folder via the FileOutputStream. Finally, the byte array was written from a specified byte array to the file output stream via FileOutputStream.write(byte[] b) API method.

In the MainActivity interface, click the historical review button to enter the historical review (ReviewCaseActivity) interface. The historical waveform interface is shown in Fig. 9.

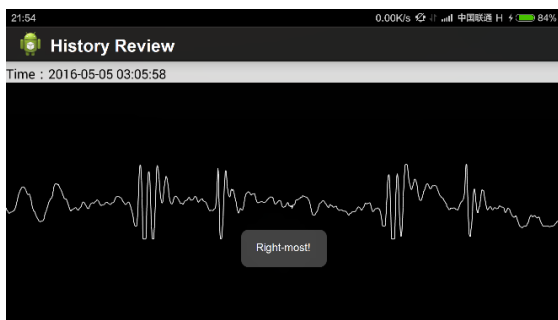


FIGURE 9. Heart sound waveform in real-time.

Moreover, the raw data stored on the smartphone could transfer to PC for further analysis. As an original signal may include intrinsic noise and possible interference signals, the pre-processing, feature extracting, and classification should be performed to get effective information.

### D. HILBERT-HUANG TRANSFORM

Heart sound signals recorded by electronic stethoscope are often encompassed with external and internal noise causing a wide frequency interference, as noise caused by motion, speech, respiration, digestion, etc. Hence pre-processing is essential. Signal segmentation is usually carried out after de-noise processing, due to the complicated raw signal waveform [29]. The diagram of heart sound processing is shown in Fig. 10.

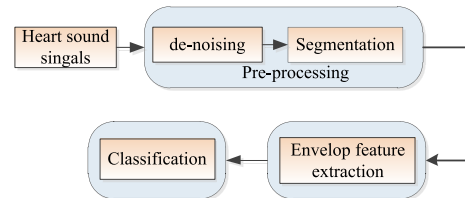


FIGURE 10. The diagram of heart sound signal processing.

The original heart sound signals may contain noises with a wide range of frequency and have non-stationary and non-linear characteristics. Common methods of signal processing include Short Time Fourier Transform(STFT), Wigner-Ville Distribution, Wavelet transform, etc. However, these signal processing methods have some limitations [31]. STFT resolution is limited either in time or frequency. The Wigner-Ville Distribution which has been applied widely in the analysis of non-stationary signals offers an excellent resolution in both frequency and time domain. However, it has a disadvantage that the cross-term interference will be introduced in the multicomponent signals. Wavelet transform has been widely used to analyze signals as a time-frequency analysis method. However, the Wavelet transform is not a self-adaptive method, and some redundant frequency will not be eliminated effectively after being firstly filtered. Therefore, considering the non-stationary and nonlinear signals, an appropriate method should be applied to analysis heart sound signals.

Hilbert-Huang transform (HHT) [32] is a time-frequency method which is widely used in speech recognition, seismic signal analysis [33], physiological signal analysis [34], etc. In recent years, many researchers have used it to analyze heart sound signals [35]. Hilbert-Huang transform consists of two parts: Empirical mode decomposition(EMD) and Hilbert transform. EMD can decompose the signal into finite and small numbers of intrinsic mode functions(IMFs) components, which is much adaptive and highly efficient. The decomposition method is appropriate for nonlinear and non-stationary signal analysis as well as for time-frequency-energy representations since the basis of expansion is adaptive. The method has a powerful capability to reveal true physical meanings for the data examined, due to its entirely empirical characteristic. The implementation of Hilbert transform on the IMF components can obtain the features of instantaneous frequency, amplitude, Hilbert spectrum, etc.

## 1) EMPIRICAL MODE DECOMPOSITION (EMD)

In the EMD process, the IMF components should meet two conditions: on the one hand, the absolute differences between extreme points and the zero crossing points is one or zero in the range of signals, on the other hand, the local mean of the maximum value of the upper envelope and the minimum value of the lower envelope should be zero.

After  $n$  times of iterative processes, the original signal  $x(t)$  could represent as

$$x(t) = \sum_{i=1}^n c_i(t) + r_n(t) \quad (1)$$

moreover,  $c_i(t)$  was one of the IMFs changing from  $c_1(t)$  to  $c_n(t)$ , and  $r_n(t)$  was the residual signal.

The process will not stop till meets the certain condition. Therefore, we should build termination criteria during the decomposition process, which specifies a standard deviation, and it denoted as  $S_d$  expressed as:

$$S_d = \sum_{i=0}^T \frac{|c_{i-1}(t) - c_i(t)|^2}{c_k^2(t)} \quad (2)$$

$T$  expressed as the time span of the signal, and the value of  $S_d$  ranges from 0.2 to 0.3 [36].

## 2) HILBERT TRANSFORM

The heart sound consists of four parts: S1, the systole, S2, the diastole. In order to exhibit the heart sound signals properly, the four parts should be highlighted via segmentation method. There are two methods to segment the signal. The first way is to use the QRS and T-waves of ECG signal [37]. However, the timing between electrical and mechanical activities is not consistent between individuals, and the T-waves is too weak to be detected in some patients. The other way is to use the envelope which reflects the amplitude of the signal. In this paper, we use the second method to segment the heart sound signals. Hilbert transform can help extracting the envelope of the signal. The procedure of this method is introduced in this section. The  $x(t)$  which is the raw data of heart sound signals acts as the real part, and the  $\hat{x}(t)$  which is the Hilbert transform results act as the imaginary part. The analytic signal of heart sound can be expressed as:

$$y(t) = x(t) + j\hat{x}(t) \quad (3)$$

The envelope of the heart sound is the amplitude of  $y(t)$ , denoted as:

$$Y(t) = |x(t) + j\hat{x}(t)| = \sqrt{x(t)^2 + \hat{x}(t)^2} \quad (4)$$

Moreover, marginal Hilbert spectrum reflects the probability that a specific frequency will occur over the entire time axis, that is to say, the cumulative number of the specific frequency occurs over the entire time axis [38]. According to Hilbert transform, the original signal could be expressed

by

$$x(t) = \sum_{i=1}^n A_i(t) \exp(j \int \omega_i(t) dt) \quad (5)$$

$A_i$  was the amplitude of the corresponding IMF, and  $n$  represented the quantity of IMFs. The summation of the real part indicated the Hilbert spectrum, which would be expressed as:

$$H(\omega, t) = \text{Re}\left\{ \sum_{i=1}^n A_i(t) \exp(j \int \omega_i(t) dt) \right\} \quad (6)$$

moreover, the marginal Hilbert spectrum was calculated as follows:

$$h(t) = \int_{-\infty}^{+\infty} H(\omega, t) dt = \int_{-\infty}^{+\infty} \sum_{i=1}^n A_i(t) \exp(j \int \omega_i(t) dt) \quad (7)$$

## IV. EXPERIMENT AND RESULTS

This research analyzed both the normal and anomaly heart sound. The normal heart sound data were collected from 10 student volunteers (Mean = 23, Std = 2.5). The written consent was acquired from each participant prior to the experimental sessions. This was a non-clinical study performed on healthy subjects without any harming procedure. Therefore, ethical approval was not sought for execution of this study. These data were collected by the proposed auscultation monitoring system, with the sampling frequency of 1kHz. The data collection environment is shown in Fig. 11, which was under the laboratory environment. The anomaly heart sound dataset from PhysioNet/Computing in Cardiology (CinC) Challenge 2016 are used to verify the accuracy of the classification [39]. 15 datasets are selected from the database. The collected datasets were uploaded to PC for further analysis. The analysis of the heart sound is discussed as follows.

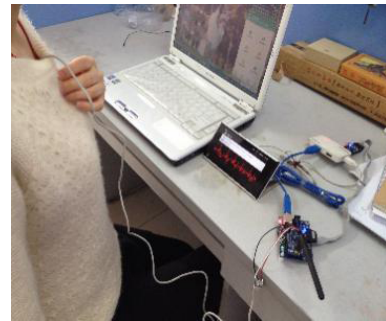
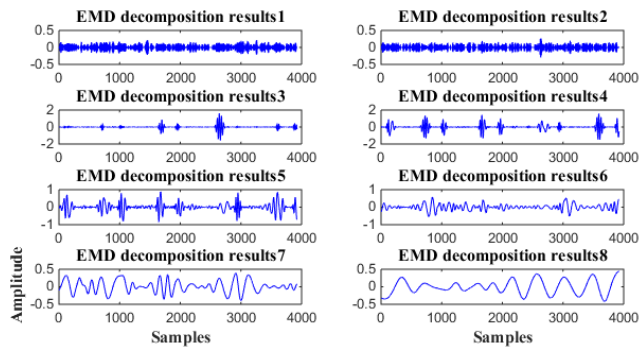


FIGURE 11. Heart sound measurement in real-time.

### A. DE-NOSING

In this paper, HHT was used to eliminate the low or high-frequency noise. The EMD process is a way to decompose a signal into multiple IMFs. According to the EMD principle, the higher of the value of  $i$  in  $c_i(t)$ , the lower of the corresponding IMF frequency is. A part of decomposition results of the original signal after EMD are shown in Fig. 12. The

number of the IMF is 8, and the residual value is not shown in this picture.



**FIGURE 12.** The decomposition results of normal heart sound.

In Fig. 12, the heart sound signal is decomposed to several IMFs according to the frequency. The figure in the upper left corner is one of the IMFs with the highest frequency. In contrast, the IMF shown in the lower right corner has the lowest frequency. As the different termination criteria, the amounts and the amplitude of IMF are different. The heart sound signal included the high frequency and the low frequency, and the useful signal of S1 and S2 is mainly concentrated between 30 to 200Hz. In order to eliminate the noise, we only need to reconstruct the IMFs between 30 to 200Hz. In general, the third to sixth of the IMFs contain the mainly useful signals. The reconstructive signal is shown in Fig. 13.

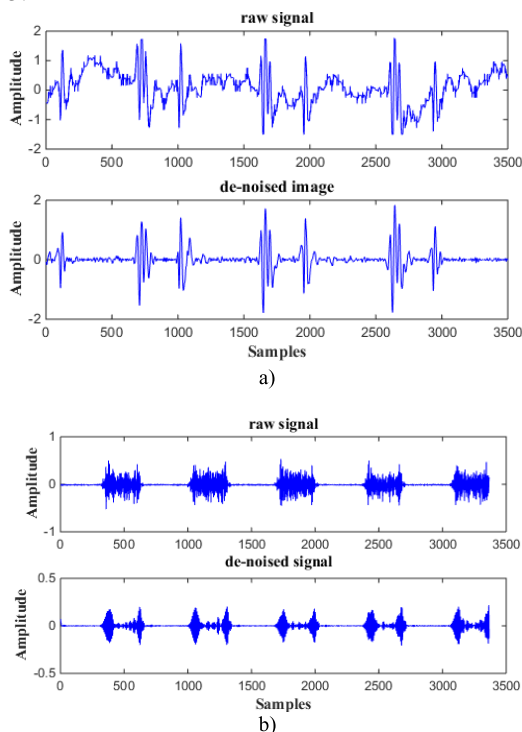


**FIGURE 13.** Heart sound EMD de-noising results. a) Normal heart sound. b) Anomaly heart sound.

**B. HEART SOUND SEGMENTATION**

Before segmentation, the heart sound envelope should be extracted. As mentioned in Hilbert Transform part,

the envelope of the heart sound is the amplitude of  $y(t)$  which is the analytic signal of heart sound signals. The heart sound envelope is shown in Fig. 14. According to Nyquist Theory, the heart sound signal was executed re-sampling, and the re-sampling frequency was set to 500Hz.

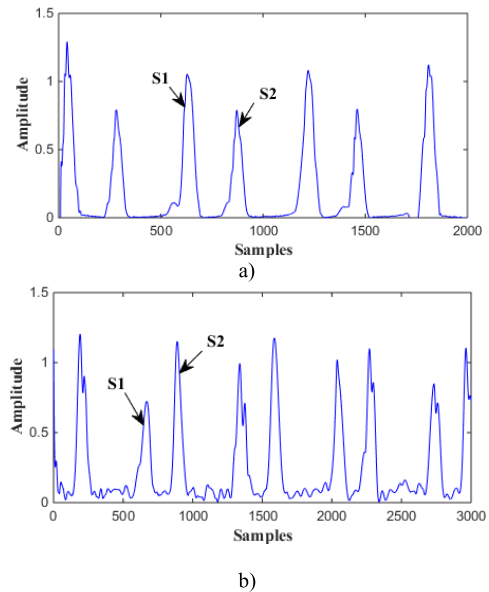


**FIGURE 14.** Heart sound envelope. a) Normal heart sound envelope. b) Anomaly heart sound envelope.

In Fig. 14, the heart sound envelope based on the S1 and S2 gives more simple and conspicuous representation than the original signals. However, the original envelope contains many burrs, which have an adverse effect on the further analysis. In this paper, cubic spline interpolation was used to remove the burrs. Segmentation of the heart sound signal is mainly to complete the recognition of S1 and S2 and determine the location of the start and end point. Many types of research adopt to set the threshold to determine the time intervals of S1 and S2. While the suitable value might be changed dependently on the personal individual or the type of pathology. Moreover, the time interval depends on the threshold, that if the threshold is too large, the interval will be short than the real one, and if the threshold is too small, the results will be influenced by the noise peaks which is large enough to be detected. So the double threshold will get higher accuracy than a single threshold. In this paper, the location of the S1 and S2 is identified by double threshold [40], [41], that the low threshold determines to detect all intervals, and that the high threshold determines to eliminate the effect of the noise.

The first step of segmentation is to extract the whole extremum points via the sliding window. The envelope curve is divided into the same duration according to the sliding window which is determined by the heart sound characteristics. The mean value  $M$  is obtained from the extremum points of each segment. The high threshold denoted as  $H$ , where

$$H = M^*a \tag{8}$$



moreover, the low threshold denoted as  $L$ , where

$$L = M^*b \quad (9)$$

The range of the value  $a$  is from 0.1 to 0.3 according to the amplitude, and  $b$  is from 0.05 to 0.1, that the threshold can adapt to individuals or different pathology. The heart sound signals vary between different people, even for the normal heart sound, and the pathological signals are complicated for combining with heart murmurs. So the threshold differs from individuals and has an effect on the accuracy of the heart sound segmentation.

Through the sliding window, find the first point which is greater than  $H$ , and stores the points into array A. The high threshold can ensure that the larger amplitude point can be detected, and can effectively avoid the smaller amplitude of noise. According to each point of array A, search for 80 data (the length of the data is determined by the frequency of signals) before and after each point respectively, and find the first point which is less than or equal to  $L$ . These points are stored in array B and C respectively, which represent the starting and ending points of S1 or S2. In order to distinguish these points from S1 and S2, it is possible to compare the difference value between the data in C array and the data in B array. Due to the duration of S1 is longer than S2, we can make a conclusion that the points belong to S1 or S2. The result of segmentation is shown in Fig. 15.

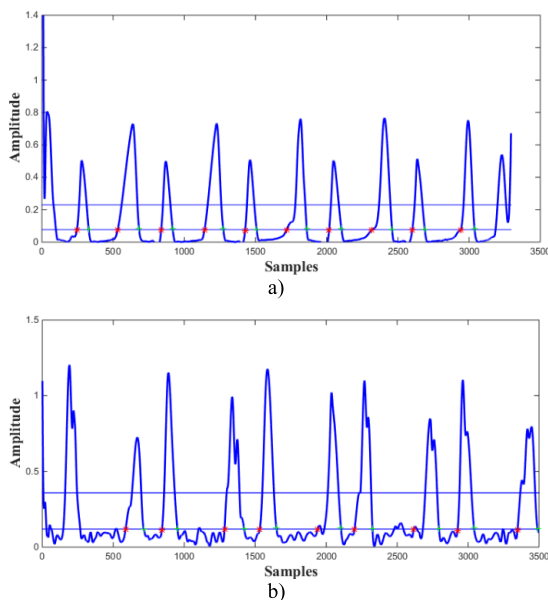


**FIGURE 15.** Heart sound segmentation results. a) Normal heart sound segmentation result. b) Anomaly heart sound segmentation result.

The detection result is shown in table 2. The total samples of S1 and S2 were 873 and 885 respectively. The normal heart sound of S1 and S2 can be entirely detected from 578 and 580 samples respectively. While the anomaly heart sound signals were influenced by the murmurs which have

more noise peaks, and the detection rate is 88.4% and 82.7% respectively.

**TABLE 2.** Detection results.

Heart Sound	Samples		Detection Rate (%)		
	Total	Normal	Anomaly	Normal	Anomaly
S1	873	578	295	100	88.4
S2	885	580	305	100	82.7

### C. WAVEFORM FEATURES EXTRACTION

Features extraction, which is the process of identifying distinctive properties from a signal, plays an important role in the effective classification of heart sound signals. In general, the features can be extracted from the time domain, frequency domain, statistical domain and time-frequency domain. In this paper, T1 (T2) indicates the interval of the first heart sound (second heart sound), and T11 exhibits the time intervals of two adjacent first heart sound which represents the heart sound circle, and T12 represents the duration from the start of first heart sound to the end of second heart sound, respectively. T1, T2, T11, and T12 extracted from the time domain according to the result of segmentation, were regarded as the features for heart sound classification. The diagram of the four parameters is shown in Fig. 16.

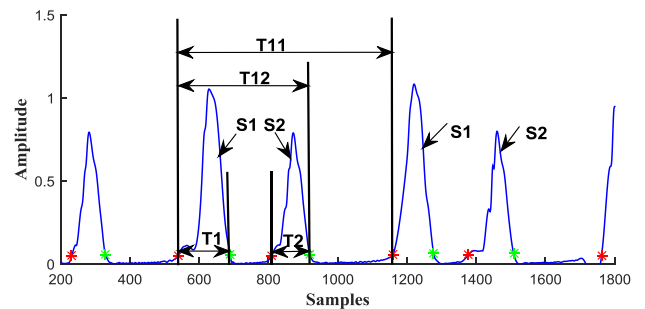


**FIGURE 16.** Definition of heart sound physiological parameters.

Furthermore, the change of heart sounds not only displays the changes in the time domain but also in the frequency domain. The Hilbert marginal spectrum of heart sound signal is shown in Fig. 17. The calculation of the Hilbert marginal spectrum has been introduced in the Hilbert Huang Transform part. According to the definition of Hilbert marginal spectrum, the cumulative number of the normal heart sound over the entire time axis is concentrated around 30-150Hz. While the frequency distribution of anomaly heart sound is larger than the former.

The difference of frequency between normal and anomaly heart sound has shown obviously in Fig. 17. The frequency of the anomaly is higher than the normal heart sound due to the appearance of murmurs. The cardiac structure would be changed when the disease happened, such as mitral stenosis, mitral insufficiency, aortic stenosis, etc. However, the specific type of disease is beyond the scope of this research.

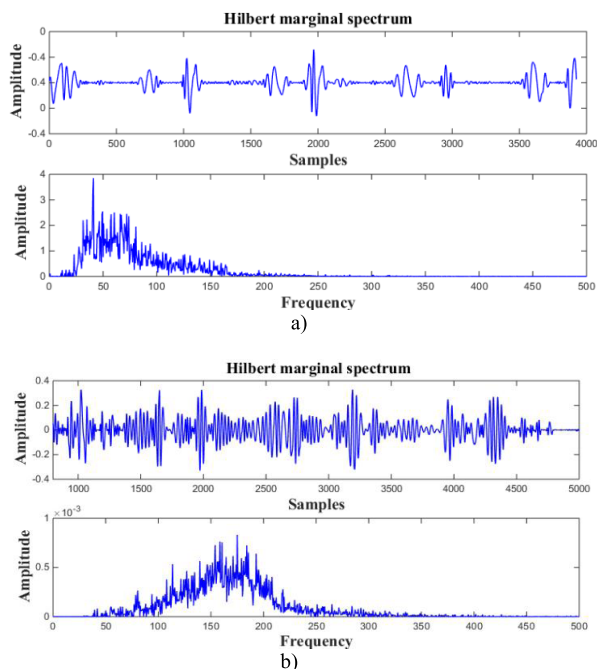


**FIGURE 17.** The Hilbert marginal spectrum of heart sound signals. a) Normal heart sound. b) Anomaly heart sound.

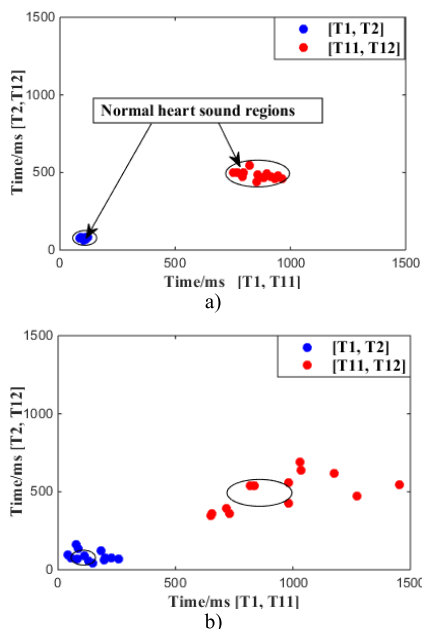


**FIGURE 18.** Two-dimensional scatter-gram for T1, T2, T11, and T12. a) Ranges of normal heart sound. b) Ranges of anomaly heart sound.

**D. DATA CLUSTERING**

In order to visualize T1, T2, T11, and T12, an easy understanding two-dimensional scatter-gram for these parameters which were extracted from normal heart sounds and anomaly heart sounds were shown in Fig. 18, respectively. According to the visualization of the extracted features, the inexperienced users are able to monitor their heart condition more easily and clearly.

In this research, the running time of the algorithm to extract time intervals of T1, T2, T11 and T12 from the data length of more than 70,000 is approximate to 1 second, applying the toolbox and functions integrated in MATLAB (computer configuration: 8G RAM, 64 bit Windows 10). Nevertheless, the running time is affected by the device performance. The computational load is beyond the scope of this research, and the implementation on the level of real time platform level will be considered in the future work.

**V. DISCUSSION**

An integrated system for heart sound acquisition, storage, asynchronous analysis has been developed. Two parameters, PLR and RSSI, were recruited to calibrate the signal transmission quality. Besides, a comparison between the normal heart sound data which were collected using our acquisition system and the normal heart sound data which were selected from PhysioNet/Computing in Cardiology (CinC) Challenge 2016 (10 cases in each group) has been done to validate the system. After being de-noised, the marginal Hilbert spectrum was used to compare the frequency ranges between the two datasets. The results showed that the frequency ranges of the heart sound signals detected by our system is among 20-170 Hz, and the frequency ranges of the heart sound signals from PhysioNet datasets is among 30-200 Hz. The small difference between the two groups may be caused by the individual differences. The results validated that our system has the capability to collect and analyze heart sound signals accurately. Additionally, this was a non-clinical study performed on healthy subjects, and the clinical test would be considered for our future research work.

In general, a normal adult heartbeat frequency is around 75 per minute, which means that the heart sound cycle is approximate 0.8 seconds. The duration of the arterial contraction or ventricular systole [T1, T2] is around 0.1 seconds, and the duration of systole and diastole T12 is about 0.4 seconds. The tilted ellipse indicated the region where the [T1, T2] and [T11, T12] data points would fall for this group of subjects [41]. The identification of the normal or anomaly heart sounds depended on the two circles. The heart sounds can be identified as normal, if the characteristic parameters [T1, T2] and [T11, T12] are belong to this two circles. Oppositely, the heart sound signal is pathological.

At present, 20 normal heart sounds from 10 healthy subjects were collected through the proposed monitoring system, and the anomaly heart sound datasets were selected from PhysioNet/Computing in Cardiology (CinC) Challenge 2016, 15 recordings in total. According to Table 2 and Fig. 18 a), the accuracy to distinguish the normal heart sound is 100%. While 13 anomaly subjects were correctly recognized from 15 anomaly subjects according to Table 3. The system algorithm evaluated the anomaly heart sound detection accuracy was 86.66%, according to Table 2 and Fig. 18 b). When some heart disease occurs, such as the valvular disease and ventricular septal defect, the duration of the systole and diastole could be changed. As we can see from Fig. 18 b),

part of the data points of anomaly heart sound was out of the nominal range, and parts of the data points were still in the nominal range which is because not all the heart disease would present abnormality both [T1, T2] and [T11, T12], such as arrhythmia which parameters [T1, T2] distributed in the normal circle [42]. However, there is no standard to ensure the center and the radius size of the nominal range, and due to the nature of non-stationary property of the heart murmurs, the anomaly heart sounds may be wrong distinguished as normal. The accuracy of the classification is influenced by the segmentation which is determined by the selection of the threshold. From Fig. 17, the frequency of normal and anomaly heart sound has an obvious distinction. Taking this into consideration, the time-frequency analysis would be considered for future research work.

**TABLE 3. Anomaly heart sound clustering results.**

Subject	[T1, T2]	[T11, T12]
Sub.1	N	A
Sub.2	A	A
Sub.3	A	N
Sub.4	N	A
Sub.5	N	A
Sub.6	A	N
Sub.7	N	N
Sub.8	N	A
Sub.9	A	A
Sub.10	N	N
Sub.11	A	N
Sub.12	N	A
Sub.13	A	A
Sub.14	A	N
Sub.15	A	N

N represents the Normal distribution of [T1, T2] or [T11, T12]. A represents the Anomaly distribution of [T1, T2] or [T11, T12].

## VI. CONCLUSION

In this paper, a new cardiac auscultation protocol has been developed, namely, Wireless Cardiac Auscultation Monitoring System. The major contribution includes the novel hardware devices with the peripheral devices wirelessly, which can access data remotely, facilitate seamless connectivity between users and clinical physiology, and provide data analysis for clinical decision support. The originality of this research includes the new wireless cardiac monitoring system for home environment and simultaneously troubleshoot the issues of noise, preprocessing, segmentation and annotation model, and the proposed prototype which has an advantage over traditional stethoscope in terms of power consumption, wireless communication, abilities of portable, power efficiency, simplify operation, and cost efficiency. The protocol is simple to configure and implement with the application of the Internet of Things. It is suitable for the home environment, predicting cardiac wellness of an inhabitant through the auscultation sound monitoring of an inhabitant. The data has been collected and analyzed through statistical logic to generate the cardiac pattern. The segmentation performance followed by feature extraction for S1 and S2 was 88.4% and

82.7% respectively in anomaly situation with the application of double-threshold. In the endeavor to build the healthcare protocol, a significant 86.66% accuracy for anomalous heart sound detection has been achieved. It is expected that the healthcare system will be further aimed to implement more experiments under different detailed anomaly heart disease, and give more accurate results. The future scope of the system is to optimize algorithms for accurate results and classify different cardiac diseases.

## REFERENCES

- [1] J. Qi, P. Yang, M. Hanneghan, and S. Tang, "Multiple density maps information fusion for effectively assessing intensity pattern of lifelogging physical activity," *Neurocomputing*, vol. 220, pp. 199–209, Jan. 2017.
- [2] Q. Wang, P. Markopoulos, B. Yu, W. Chen, and A. Timmermans, "Interactive wearable systems for upper body rehabilitation: A systematic review," *J. Neuroeng. Rehabil.*, vol. 14, Mar. 2017, Art. no. 20.
- [3] Q. Wang et al., "Smart rehabilitation garment for posture monitoring," in *Proc. 37th Annu. Int. Conf. IEEE Eng. Med. Biol. Soc.*, Aug. 2015, pp. 5736–5739.
- [4] C. Zou, Y. Qina, C. Sun, W. Li, and W. Chen, "Motion artifact removal based on periodical property for ECG monitoring with wearable systems," *Pervasive Mobile Comput.*, vol. 40, pp. 267–278, Sep. 2017.
- [5] G. Elhayatmy, N. Dey, and A. S. Ashour, Eds., "Internet of Things based wireless body area network in healthcare," in *Internet of Things and Big Data Analytics Toward Next-Generation Intelligence*. Springer, 2018.
- [6] J. H. Abawajy and M. M. Hassan, "Federated Internet of Things and cloud computing pervasive patient health monitoring system," *IEEE Commun. Mag.*, vol. 55, no. 1, pp. 48–53, Jan. 2017.
- [7] H. Ghayvat, S. Mukhopadhyay, X. Gui, and N. Suryadevara, "WSN- and IoT-based smart homes and their extension to smart buildings," *Sensors*, vol. 15, no. 5, pp. 10350–10379, 2015.
- [8] J. Qi, P. Yang, M. Hanneghan, D. Fan, Z. Deng, and F. Dong, "Ellipse fitting model for improving the effectiveness of life-logging physical activity measures in an Internet of Things environment," *IET Netw.*, vol. 5, no. 5, pp. 107–113, Sep. 2016.
- [9] J. Qi, P. Yang, G. Min, O. Amft, F. Dong, and L. Xu, "Advanced Internet of Things for personalised healthcare systems: A survey," *Pervasive Mobile Comput.*, vol. 41, pp. 132–149, Oct. 2017.
- [10] S. Yuenyong, A. Nishihara, W. Kongprawechnon, and K. Tungpimolrut, "A framework for automatic heart sound analysis without segmentation," *Biomed. Eng. Online*, vol. 10, p. 13, Feb. 2011.
- [11] A. T. Dao, "Wireless laptop-based phonocardiograph and diagnosis," *PeerJ*, vol. 3, no. 3, p. e1178, 2015.
- [12] R. E. Pérez-Guzmán, R. García-Bermúdez, F. Rojas-Ruiz, A. Céspedes-Pérez, and Y. Ojeda-Riquenes, "Evaluation of algorithms for automatic classification of heart sound signals," in *Proc. Int. Conf. Bioinf. Biomed. Eng.* Cham, Switzerland: Springer, 2017, pp. 536–545.
- [13] S. Leng, R. S. Tan, K. T. C. Chai, C. Wang, D. Ghista, and L. Zhong, "The electronic stethoscope," *Biomed. Eng. Online*, vol. 14, p. 66, Jul. 2015.
- [14] D. Tosi, M. Olivero, and G. Perrone, "Low-cost fiber Bragg grating vibroacoustic sensor for voice and heartbeat detection," *Appl. Opt.*, vol. 47, no. 28, pp. 5123–5129, 2008.
- [15] Y. Hu and Y. Xu, "An ultra-sensitive wearable accelerometer for continuous heart and lung sound monitoring," in *Proc. Eng. Med. Biol. Soc. Conf.*, Aug./Sep. 2012, p. 694.
- [16] S. Rajala and J. Lekkala, "Film-type sensor materials PVDF and EMFi in measurement of cardiorespiratory signals—A review," *IEEE Sensors J.*, vol. 12, no. 3, pp. 439–446, Mar. 2012.
- [17] G. Zhang, M. Liu, N. Guo, and W. Zhang, "Design of the MEMS piezoresistive electronic heart sound sensor," *Sensors*, vol. 16, no. 11, p. 1728, 2016.
- [18] Z. Zhao, Z. Zhao, and Y. Chen, "Time-frequency analysis of heart sound based on HHT [Hilbert-Huang transform]," in *Proc. IEEE Int. Conf. Commun., Circuits Syst.*, May 2005, p. 929.
- [19] T.-H. Hung et al., "Time-frequency analysis of heart sound signals based on Hilbert-Huang Transformation," in *Proc. IEEE, Int. Symp. Consum. Electron.*, Jun. 2012, pp. 1–3.
- [20] M. A. Kot et al., "Improving the recognition of heart murmur," *Int. J. Adv. Comput. Sci. Appl.*, vol. 7, no. 7, pp. 283–287, 2016.

- [21] Littman Company. Accessed: Jan. 15, 2017. [Online]. Available: [http://www.littmann.com/3M/en\\_US/littmann-stethoscopes/](http://www.littmann.com/3M/en_US/littmann-stethoscopes/)
- [22] Thinklabs One Digital Stethoscope. Accessed: Jan. 15, 2017. [Online]. Available: <http://www.thinklabs.com/>
- [23] Eray Medical Supplies Inc. Accessed: Mar. 20, 2018. [Online]. Available: <http://www.eraymedical.com/3mli41elstbl.html>
- [24] C. Samjin, "Heart sound measurement and analysis system with digital stethoscope," in *Proc. Asia Int. Symp. Mechatronics*, 2008, pp. 1–5.
- [25] Z. Zhao and S. He, "A heart sound transmission and reception system based on NFC and bluetooth," in *Proc. Int. Conf. Health Inform.* Springer, 2014, pp. 187–190.
- [26] A. Leatham, *Auscultation of the Heart and Phonocardiography*. London, U.K.: Churchill Livingstone, 1975.
- [27] D. B. Springer, L. Tarassenko, and G. D. Clifford, "Logistic regression-HSMM-based heart sound segmentation," *IEEE Trans. Biomed. Eng.*, vol. 63, no. 4, pp. 822–832, Apr. 2016.
- [28] Huake Electronic Technology Research Institute. Accessed: Jan. 15, 2017. [Online]. Available: <http://hfhuaque.tecenet.com/mall/itemid-3287.shtml>
- [29] Texas Instruments. (Oct. 2010). *CC2540 Datasheet*. [Online]. Available: <http://www.ti.com/lit/ds/symlink/cc2540.pdf>
- [30] A. K. Abbas and R. Bassam, "Phonocardiography signal processing," in *Synthesis Lectures on Biomedical Engineering*, vol. 4. California, CA, USA: Morgan & Claypool, 2009, p. 218.
- [31] Y.-L. Tseng, P.-Y. Ko, and F.-S. Jaw, "Detection of the third and fourth heart sounds using Hilbert–Huang transform," *Biomed. Eng. OnLine*, vol. 11, Feb. 2012, Art. no. 8.
- [32] N. E. Huang *et al.*, "The empirical mode decomposition and the Hilbert spectrum for nonlinear and non-stationary time series analysis," *Proc. R. Soc. Lond. A, Math. Phys. Sci.*, vol. 454, no. 1971, pp. 903–995, 1998.
- [33] Z. X. Chen, W. U. Chen, and R. Z. Zhou, "Hilbert-Huang transform spectrum and its application in seismic signal analysis," *J. Fuzhou Univ.*, vol. 34, no. 2, pp. 260–264, 2006.
- [34] N. E. Huang and S. S. P. Shen, *Hilbert–Huang Transform and its Applications*. Singapore: World Scientific, 2005.
- [35] A. Altamirano-Altamirano, A. Vera, L. Leija, and D. Wolf, "Myoelectric signal analysis using Hilbert–Huang Transform to identify muscle activation features," in *Proc. Int. Conf. Elect. Eng., Comput. Sci. Autom. Control.*, Sep. 2016, pp. 1–4.
- [36] N. E. Huang and Z. Wu, "A review on Hilbert–Huang transform: Method and its applications to geophysical studies," *Rev. Geophys.*, vol. 46, no. 2, p. RG2006, 2008.
- [37] M. B. Malarvili, I. Kamarulafizam, S. Hussain, and D. Helmi, "Heart sound segmentation algorithm based on instantaneous energy of electrocardiogram," in *Proc. Comput. Cardiol.*, Sep. 2003, pp. 327–330.
- [38] H. Wang, J. Chen, Y. Hu, Z. Jiang, and C. Samjin, "Heart sound measurement and analysis system with digital stethoscope," in *Proc. IEEE Int. Conf. Biomed. Eng. Inform.*, Oct. 2009, pp. 1–5.
- [39] C. Liu *et al.*, "An open access database for the evaluation of heart sound algorithms," *Physiol. Meas.*, vol. 37, no. 12, pp. 2181–2213, 2016.
- [40] J. Chen and H. Hou, "Segmentation of heart sound using double-threshold," in *Proc. 5th Int. Conf. Meas. Technol. Mechatronics Automat.*, Jan. 2013, pp. 985–988.
- [41] X. Guo, H. Lin, and S. Xiao, "Medical parameters extraction of heart sounds," *Comput. Eng. Appl.*, vol. 47, no. 3, pp. 214–217, 2011.
- [42] Z. Jiang and S. Choi, "A cardiac sound characteristic waveform method for in-home heart disorder monitoring with electric stethoscope," *Expert Syst. Appl.*, vol. 31, no. 2, pp. 286–298, 2006.